



# Preparation and characterization of bacterial cellulose by kombucha using corncob

Zhanna Liu · Qihang Sun · Yingying Wang · Jie Liu · Ping Zhu

Received: 19 June 2023 / Accepted: 17 June 2024 / Published online: 22 June 2024  
© The Author(s), under exclusive licence to Springer Nature B.V. 2024

**Abstract** Bacterial cellulose (BC) is widely used in various fields due to its excellent physicochemical properties. However, the main drawback is its high production cost. The present research exploited the preparation of BC by combining the hydrothermal process using acetic acid and enzyme treatment for the hydrolysis of corncob. The BC production was further improved by optimizing the key factors. The concentration of reducing sugar was 22.7 g/L after thermohydrolysis at 180 °C for 80 min and enzyme hydrolysis in 6 U/mL cellulase buffer solution for 24 h. It supported about 1.36 g/L as the sole culture medium, which was 5.6 times more than corncob hydrolysate without detoxification (0.25 g/L) and more than Hestrin-Schramm (HS) standard medium

(1.12 g/L). The BC products were characterized by FT-IR spectroscopy, XRD, TG, and SEM analysis. Compared to the BC produced by HS medium, the morphology of BC produced by detoxification corncob hydrolysate showed a lower value of the coefficient of variation (37.59%) and higher mean diameter (55.23 nm). XRD data showed higher crystallinity (77.50%) and TG analysis showed high thermal stability. The current study demonstrated that corncob is a promising carbon source for the sustainable production of BC.

**Keywords** Bacterial cellulose · Corncob · Kombucha · Hydrolysis · Hydrothermal process

---

Z. Liu · Q. Sun · J. Liu (✉) · P. Zhu (✉)  
College of Textile and Clothing, Institute of Functional Textiles and Advanced Materials, State Key Laboratory of Bio-Fibers and Eco-Textiles, Qingdao University, Ningxia Road 308, Qingdao 266071, Shandong, China  
e-mail: jliu0411@163.com

P. Zhu  
e-mail: pzhou99@163.com

Z. Liu · Y. Wang  
Zibo Key Laboratory of Bio-Based Textile Materials, Shandong Vocational College of Light Industry, Mishan Road 30, Zibo 255300, Shandong, China

J. Liu  
Haima Carpet Group Co., Ltd, Weihai 264200, Shandong, China

## Introduction

The production of natural biopolymers and their application as biodegradable materials are green chemical and biotechnological methods, which can improve the efficiency of traditional technology and help in environmental protection (El-Gendi et al. 2023). Cellulose is a three-dimensional (3D) network polymer, consisting of glucose units, which are connected by  $\beta$ -1, 4 glycosidic bonds. Each repeating glucose unit has three hydroxyl groups, which render cellulose hydrophilic, biodegradable, and functionalizable (Choi et al. 2022). Meanwhile, cellulose is one of the most abundant and eco-friendly natural biopolymers and it can be categorized into

two types according to the source: plant-based cellulose (PC) and bacterial cellulose (BC) (Kumar et al. 2019). PC is mainly obtained from wood and agricultural waste (sugar cane, rice wheat, wheat straw) (Babaei-Ghazvini et al. 2024). In this case, it is vital to remove hemicellulose, lignin, and other impurities wrapped together in PC for application, which would involve harsh processes that cause environmental pollution (El-Gendi et al. 2022). BC is obtained from a variety of bacterial strains belonging to *Gluconacetobacter*, *Sarcina*, and *Aerobacter* genera, but kombucha with a relatively high capacity to produce cellulose, could be a good candidate for fundamental and applied research (Leonarski et al. 2021). In comparison to PC (Guo et al. 2023), BC has the advantages of high purity, strength, crystallinity, biocompatibility, and large specific surface area. Hence, BC has been widely applied in medicine (Yuan et al. 2020), food packaging (Chen et al. 2022), paper (Chen et al. 2023), cosmetics (Mbituyimana et al. 2021), and electronics (Luo et al. 2022). However, the high production cost of BC has limited its wide scope of academic studies and commercial applications (El-Gendi et al. 2023). The cost of medium accounts for about 30% of the total BC production cost. Hence, several industrial and agricultural wastes have been tested as alternative media for BC production, which include pecan nutshell (Dorame-Miranda et al. 2019), potato peel waste (Abdelraof et al. 2019), orange peel waste (Padmanabhan et al. 2022), and distillery effluent (Jahan et al. 2018). Maize is the second most produced crop worldwide, with 1.1 billion metric tons produced in 2021. This accounts for 21% of the global crop production between 2000 and 2019, wherein the corncob was about 5.6% of the entire grain harvested, that is, 61.6 million metric tons (Jesus et al. 2023). However, corncob is generally less utilized and most of it is burned directly, leading to haze, which is one of the most troublesome environmental issues and waste of resources (Zhang et al. 2023). Corncob has also been converted into high-value products, such as furfuryl alcohol and xylitol (Pan et al. 2022; Yuan et al. 2023). Although corncob has been used for the production of many chemicals, there has been limited research on their potential use as a substrate for BC production. Therefore, this study evaluates the possibility of using corncobs as a matrix for the production of BC.

Meanwhile, current academic research has focused on innovative and sustainable methods to reuse biomass residues. The hydrothermal technique is commonly used to pretreat lignocellulosic raw materials, which destroy the material structure, promotes the hydrolysis of hemicellulose, and improves the accessibility of cellulose (Sieborg et al. 2020). Mineral acid has been widely used in the hydrothermal process, due to its high catabolic activity (Chen et al. 2016). However, the use of mineral acid has many disadvantages, which include the corrosion of equipment and the generation of sewage. Acetic acid has the characteristics of recyclability and low acidity that can prevent water pollution and further assist in the subsequent process (Wen et al. 2021; Zhao et al. 2023). Most of the corncob hemicellulose can be hydrolyzed by hydrothermal treatment using acetic acid, but complete degradation of cellulose cannot be achieved (Guo et al. 2021). To maximize the utilization of corncob to produce sugars, cellulase was further added to hydrolyze the corncob for BC preparation. This paper reports a green and highly efficient synthesis of corncob hydrolysate. Thus, the aim was to achieve the production of BC through effective hydrolysis. The morphology, structural properties, and thermostability of BC prepared from a corncob culture medium were also studied.

## Materials and methods

### Hydrolysis of corncobs

Corncob hydrolysate was obtained by hydrolysis using acetic acid and cellulase. The factors that mainly affected further fermentation were the concentration of reducing sugar, furfural, 5-hydroxymethylfurfural (HMF), lignin, and cellulase, as well as the temperature and time of acid hydrolysis and enzyme hydrolysis. Corncob (5 g) was immersed in 50 mL of 2% (w/v) acetic acid and treated at 100, 120, 140, 160, 180, and 200 °C under high pressure for 20, 40, 60, 80, and 100 min to optimize the acid hydrolysis process for hydrolysate preparation. The corncob residue obtained under optimal conditions of acid pretreatment was washed three times to neutral with 1000 ml deionized water at room temperature for the next enzymatic hydrolysis.

Commercial cellulase enzyme (64,001,132, Sinopharm Chemical Reagent Co., Ltd, China) was used for enzymatic hydrolysis. The activity of endoglucanase was 1225 U/g enzyme analyzed using carboxymethyl cellulose sodium salt (CMCNa) as substrate. The activity of exoglucanase was 310 U/g enzyme measured using avicel as a substrate.  $\beta$ -glucosidase activities were 4022 U/g enzyme measured using pNPG (p-nitrophenyl  $\beta$ -D-glucopyranoside) (Jung et al. 2015).

The effect of enzyme loading on reducing sugar concentration in enzymatic hydrolysis process was investigated. Enzymatic hydrolysis was conducted using 5.5 g pretreated corncob residue and various enzyme loadings (2, 4, 6, 8, 10, 12, and 14 U/mL) in 50 mL citric acid-sodium citrate buffer solution (0.1 mol/L, pH=5.0) at 50 °C for 48 h.

To investigate the effect of enzymatic time on the reducing sugar concentration of hydrolysate, enzymatic hydrolysis was conducted using 5.5 g pretreated corncob residue, 6 U/ml cellulase in 50 mL cellulase buffer solution at 50 °C for various time (6, 12, 18, 24, 30, 36, 42, and 48 h). The acid hydrolysate and enzyme hydrolysate prepared under optimal conditions were mixed in a volume ratio of 1:1 and treated with 2% activated carbon (AC) at 40 °C for 0.5 h to remove lignin, furfural, and HMF in the preparation of the corncob culture medium.

### Production of BC

The kombucha starter culture (obtained from Shandong Ruyun Edible Fungus Planting Co. Ltd., Liaocheng, China.) consists of tea fungus (symbiotic culture of yeasts, acetic acid bacteria and lactic acid bacteria), fermented broth, cellulosic layer and teabag (5 g black tea). The activation of kombucha starter culture was slightly adjusted compared to previous studies (Aung and Eun 2021; Sharma and Bhardwaj 2019). 100 g sucrose was added to 1 L water and boiled, then 5 g black tea teabag (purchased from Hubei Picking Flower Tea Industry Co., LTD) was added. After 5 min, the infused teabag was removed. The tea fungus, fermented broth and cellulosic layer were added to the sugar-tea water cooled to 30 °C. The mixture was placed in an incubator and fermented at 30 °C for 15 days for subsequent experiments.

10% (V/V) inoculation volume of the kombucha strain was added into Hestrin-schramm medium,

corncob hydrolysate medium without AC detoxification and corncob hydrolysate medium with AC detoxification separately, then cultured at room temperature for 15 d statically. Hestrin-Schramm medium was used as the standard control, whereas corncob hydrolysate medium without and with AC detoxification was used as experimental groups to study the effect of medium type on BC yield. After fermentation, the BC membrane was treated with 0.1 mol L<sup>-1</sup> sodium hydroxide solution in an 80 °C water bath for 60 min to remove the remaining bacteria and culture medium. It was then freeze-dried in a -80 °C refrigerator for 24 h. Figure 1 summarizes the process for the preparation of BC samples in this study and the annual yield of corncob was obtained from the previous publications (Li et al. 2015; Wang et al. 2016) and industry report online (Chinafeed 2022). BC production was recorded as the dry weight of BC within the volume of the medium, according to the following equation:

$$\text{BC production (g/L)} = \frac{m \text{ (g)}}{V \text{ (L)}} \quad (1)$$

where *m* was the dry weight of BC, and *V* was the volume of the medium for BC production.

### Analysis of constituents of corncob and corncob hydrolysate

The main components of corncob were determined according to the procedure of “Determination of Structural Carbohydrates and Lignin in Biomass” (NREL/TP-510-42618) (Liu et al. 2020). The concentrations of glucose, cellobiose, xylose, arabinose, furfural, and HMF were determined by HPLC, which was equipped with an 87-H column and RID (Agilent 1200, USA). The mobile phase used was 0.02 M sulfuric acid at a flow rate of 0.6 mL min<sup>-1</sup>. The column temperature was 50 °C and the detector temperature was 45 °C.

The reducing sugar content of corncob hydrolysate was determined colorimetrically using 3, 5 dinitro salicylic acid (DNS) (Miller 1959). The absorbances were recorded at 540 nm using a UV-VIS spectrophotometer (UV-2700, Japan).

The lignin content was estimated by determining the polyphenol content by the Folin-phenol reagent method (Way et al. 2020). The absorbances were

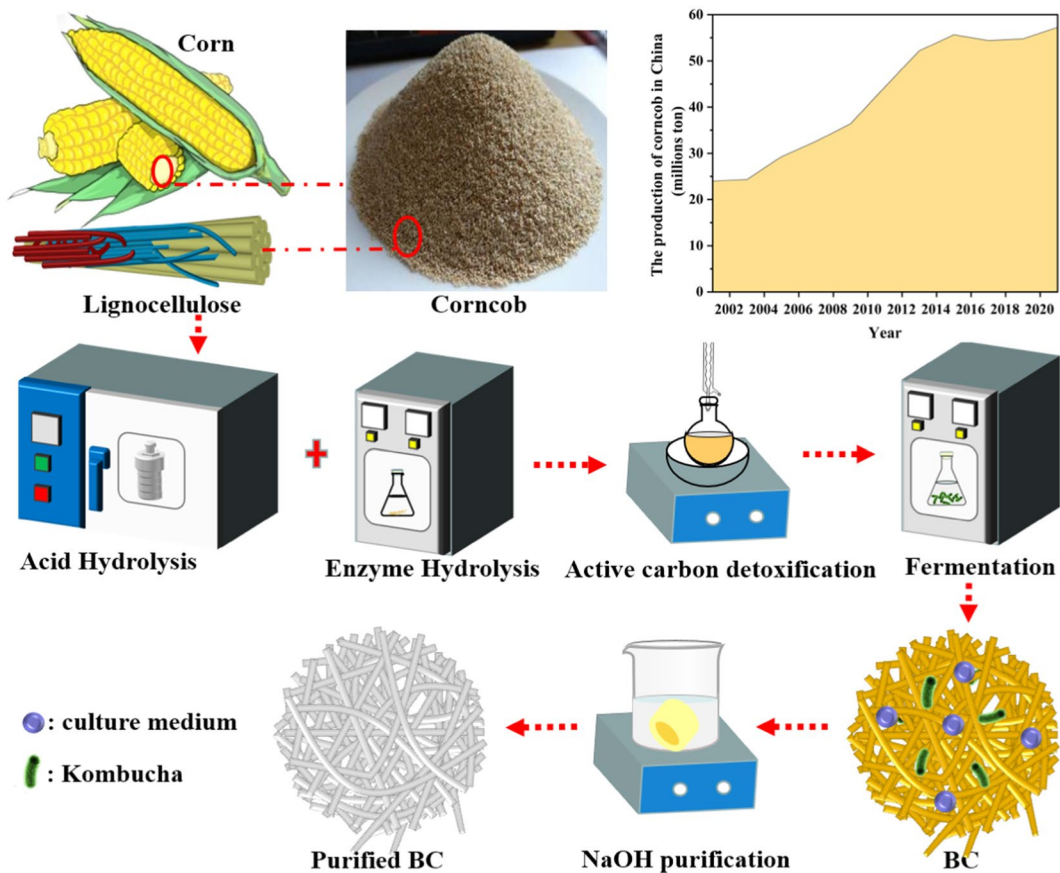


**Fig. 1** Schematic representation of the process for the preparation of BC

recorded at 765 nm using a UV-VIS spectrophotometer (UV-2700, Japan).

#### Scanning electron microscopy (SEM)

The morphological analysis of BC was conducted by SEM (JSM-6390LV, Japan). The BC sample was cut into small pieces and fixed on the sample plate with a conductive adhesive, then coated with gold and observed at 10 kV voltage under high-vacuum conditions.

#### Fourier transform infrared (FTIR)

The functional groups present in BC were examined by FTIR (Thermo Fisher Scientific, USA) in the wavelength region of 4000 to 500  $\text{cm}^{-1}$ . Data were

acquired on a Nicolet iS 50 FTIR spectrometer in the ATR mode at a resolution of 4  $\text{cm}^{-1}$ .

#### $^{13}\text{C}$ solid-state nuclear magnetic resonance ( $^{13}\text{C}$ NMR) spectroscopy

Solid-state  $^{13}\text{C}$  CP/MAS NMR spectra were recorded on an Agilent 600 DD2 spectrometer (Agilent, USA, magnetic field strength 14.1 T) at the resonance frequency of 150.72 MHz using the cross-polarization (CP), magic-angle spinning (MAS), and high-power 1 H decoupling methods. Samples in the form of powder were placed in a pencil-type zirconia rotor of 4.0 mm o.d. The spectra were obtained at a spinning speed of 10 kHz (4.2  $\mu\text{s}$  90° pulses), a 2 ms CP pulse, and a recycle delay of 3 s. The carbon signal of tetramethylsilane (TMS) at 0 ppm was used as the reference for the  $^{13}\text{C}$  chemical shift.

## X-ray diffraction (XRD) analysis

The crystal structure analysis of BC was conducted by XRD (SHI-MADZU, Japan). The BC sample was placed on a sample plate and measured in the range of  $5^\circ - 40^\circ$  at the speed of  $4^\circ \text{min}^{-1}$ . The diffraction profile was processed by Origin fitting analysis and transformed to basic crystallographic features: d-spaces of equatorial lattice planes. The interplanar distance of crystallographic planes (d-spacing) was calculated by Bragg's law. The crystallinity was calculated according to the following expression:

$$\text{CI (\%)} = 100 \times \frac{I_{200} - I_{\text{am}}}{I_{200}} \quad (2)$$

where  $I_{200}$  was the maximum intensity of the crystalline peak lattice diffraction (at about  $2\theta = 22.5^\circ$  for cellulose I) and  $I_{\text{am}}$  was the intensity of amorphous part diffraction (at about  $2\theta = 18^\circ$  for cellulose I) (Segal et al. 1959).

## Viscosity measurement and determination of degree of polymerization (DP)

The viscosity of BC was determined using an Ubbelohde viscometer. The freeze-dried samples were dissolved in copper (II) ethylenediamine solution and immersed in a water bath at a constant temperature ( $25 \pm 0.5^\circ \text{C}$ ). The degree of polymerization was calculated from the viscosity values according to (Andritsou et al. 2018).

## Thermal analyses by thermogravimetry (TG) and derivative thermogravimetry (DTG)

The thermal stability of BC was tested by TG analysis (TGA5500, USA), wherein about 4 mg of BC sample

was loaded in an alumina crucible. The sample was heated from  $30^\circ \text{C}$  to  $750^\circ \text{C}$  at a rate of  $10^\circ \text{C min}^{-1}$  under a nitrogen atmosphere.

## Results and discussion

### Chemical composition of corncob

Generally, lignocellulosic corncob contains polysaccharides, lignin, and ash. Further, cellulose contains glucan, whereas hemicellulose contains xylan and arabinan, which can be degraded into sugars under certain conditions. As seen from Table 1, corncob contained the highest amount of glucan (35.06%), as compared with other components. This indicated that it contained more cellulose than other components. Moreover, the xylan, lignin, and ash contents were higher, which were 21.98%, 15.46%, and 13.04%, respectively. The arabinan content was comparatively lower. The higher contents of hemicellulose and cellulose in corncob guaranteed the generation of a higher content of sugars in the subsequent hydrolysis process.

### Optimization of corncob hydrolysate

Figure 2 shows the effects of temperature and time of acetic acid hydrolysis of corncob. The removal rate of corncob increased with an increase in temperature (Fig. 2a). The reason was that with an increase in temperature the hydrolysis reaction of corncob intensified (Joshi and Gogate 2020). Cellulose and hemicellulose were degraded into monosaccharides or oligosaccharides, whereas lignin disintegrated totally into phenols under acidic conditions along with high temperature and pressure (Fig. 4) (Feng et al. 2017; French 2017; Liu et al. 2017b). Therefore, the

**Table 1** Chromatogram data of CC composition measured by HPLC and the main components of CC

Sugar types	HPLC chromatogram data (g/L)	Component <sup>a</sup>	Composition (%)	Component <sup>a</sup>	Composition (%)
Glucose	$1.36 \pm 0.01$	Glucan	$35.06 \pm 0.11$	Acid soluble lignin	$2.00 \pm 0.01$
Cellobiose	0				
Xylose	$0.86 \pm 0.01$	Xylan	$21.98 \pm 0.18$	Acid insoluble lignin	$13.46 \pm 0.44$
Arabinose	$0.15 \pm 0.01$	Arabinan	$3.69 \pm 0.12$	Ash	$13.04 \pm 1.11$

<sup>a</sup>The values presented are mean of three values ( $n=3$ )  $\pm$  standard deviation



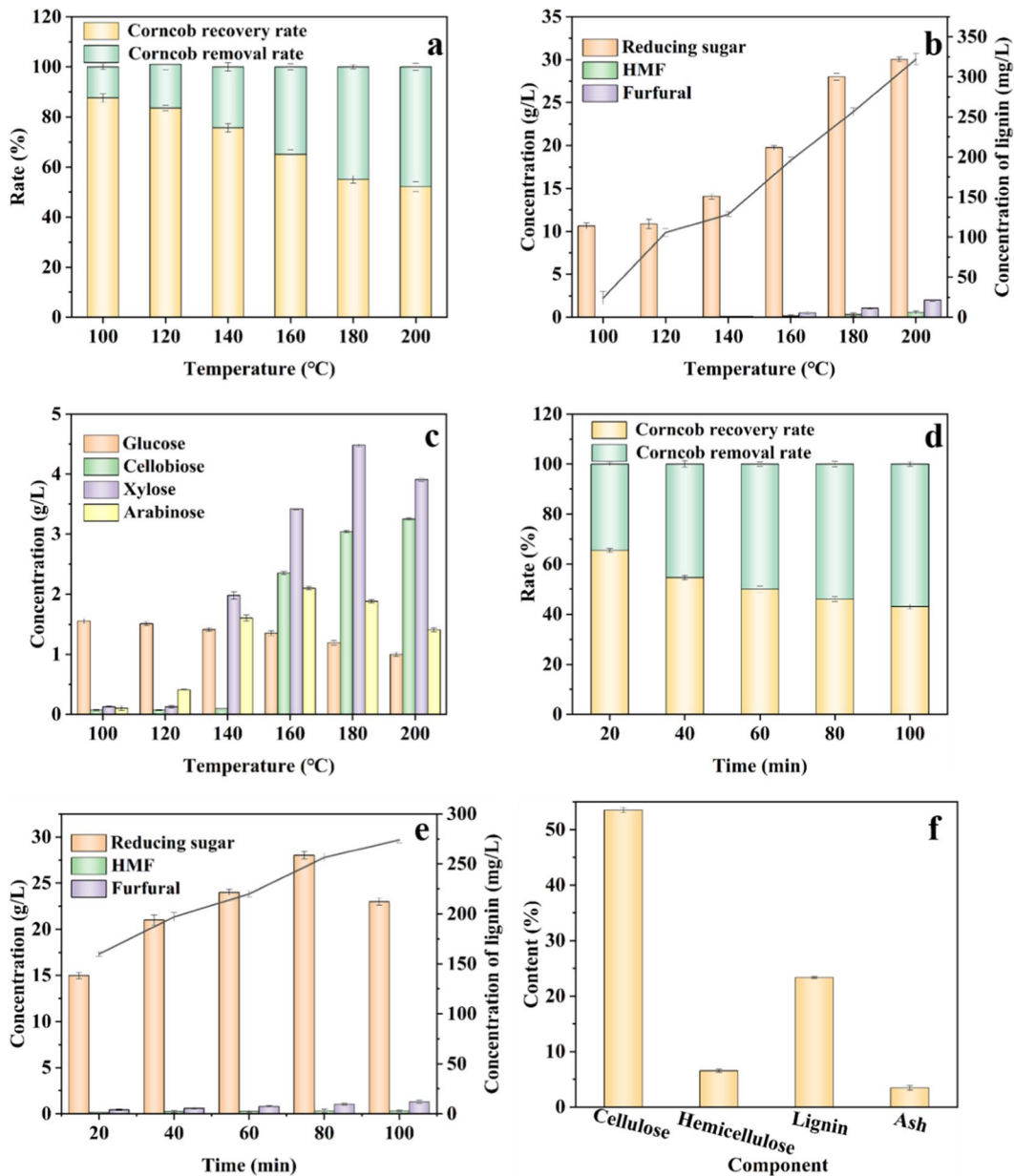


**Fig. 2** Effects of temperature and time of acetic acid hydrolysis on corncob. **a** removal and recovery rates of corncob at different temperatures; **b** the main chemical constituents in hydrolysate at different temperatures; **c** contents of main sug-

ars in the hydrolysate at different temperatures; **d** removal and recovery rates of corncob at different times; **e** the main chemical constituents in hydrolysate at different times; **f** components of corncob under optimized conditions of temperature and time

reducing sugar and phenols contents in the corncob hydrolysate increased with an increase in temperature (Fig. 2b). When the temperature reached 160 °C, furfural was produced in the hydrolysate and furfural content increased as the temperature increased. This was because the extent of conversion of arabinose

and xylose into furfural increased at high-temperature (Ouyang et al. 2023). This was also consistent with the obvious decrease in arabinose and xylose contents when the temperature exceeded 180 °C (Fig. 2c). When the reaction time reached 80 min, the reducing sugar content was maximum (28 g/L). With a further

increase in reaction time, the content of reducing sugar decreased (Fig. 2e). The reason was that up to 80 min, the cellulose and hemicellulose in the corncob underwent maximum hydrolysis. This was consistent with no obvious change in the removal rate of the corncob beyond 80 min (Fig. 2d). With the further prolongation of time, the glucose, xylose, and arabinose sugars in the hydrolysate was converted to HMF and furfural, which resulted in a decreased reducing sugar content (Nayebi et al. 2023). Therefore, pretreatment conditions of corncob at 180 °C for 80 min were optimal, with a relatively high reducing sugar content of 28 g/L and low contents of furfural 1.3 g/L and lignin 256.5 mg/L. Meanwhile, acetic acid, as a weak acid, is recyclable, easy to handle and store, and less corrosive to process equipment. Also, acid pretreatment of lignocellulosic biomass by hydrothermal process has been scale-up applied (Lee et al. 2011).

Thus, pretreatment of corn cob with 2% acetic acid has the prospect of large-scale production. Finally, the hemicellulose content in corncob was reduced to 6.52%, whereas the cellulose content increased up to 53.52% (Fig. 2f), which was convenient for a further hydrolysis reaction using cellulase.

From Table 1; Fig. 2f, it was evident that some portion of hemicellulose was removed from the corncob after acetic acid hydrolysis, which destroyed the structure of the corncob. Hence, cellulase could react more easily with the cellulose in corncob and degrade it into glucose by enzymic hydrolysis (Ma et al. 2018).

Figure 3 shows the effects of enzyme load and time on enzymatic hydrolysis of pretreated corncob. The concentration of reducing sugar increased gradually in a certain enzyme load and time and tended to be stable (Fig. 3a and c). This was because more

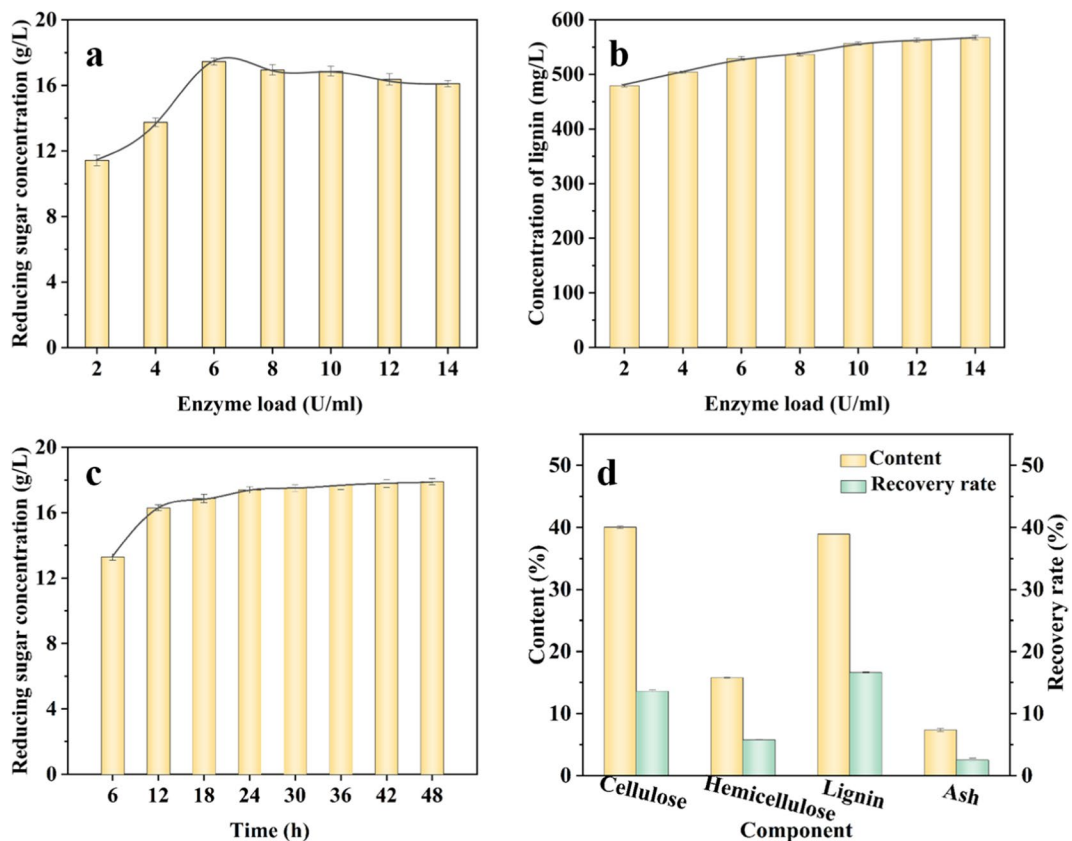


**Fig. 3** Effects of enzyme load and time on enzymatic hydrolysis of corncob. **a, b** the concentration of reducing sugar and lignin of hydrolysate with different enzyme loads; **c** the concentration

of reducing sugar of hydrolysate at different times; **d** different components and their recovery rates from corncob under optimized conditions of temperature and time

cellulose could be hydrolyzed in the pretreated corncob with the increase of enzyme load and time, and the exposed cellulose of the substrate completely reacted as the enzyme load and hydrolysis time reached 6 U/ml and 24 h, respectively. The concentration of lignin in enzymatic hydrolysate ranged from 480 to 560 mg/L with enzyme load increasing (Fig. 3b). The reason for lignin presented in enzymatic hydrolysate may be that the thermal pretreatment severity could result in the formation of soluble lignin-derived phenolic compounds. The cellulose content in corncob decreased with the increase of enzyme load, which exposed more lignin-derived polyphenol complex causing an increase in the amount of lignin small molecules in the enzymatic hydrolysate (Yuan et al. 2021). After the acetic acid pretreatment, the corncob was treated with 6 U/mL cellulase for 24 h to achieve a maximum reducing sugar concentration of about 17.4 g/L. The hemicellulose and cellulose contents of corncob were 15.7% and 39.9%, respectively, and their respective recovery rates reached 15.76% and 40.02% under optimized

pretreatment conditions (Fig. 3d). The incomplete hydrolysis of hemicellulose and cellulose could be attributed to the lignin present around the corncob, owing to which the hemicellulose and cellulose wrapped in the corncob were not fully accessible to acetic acid solution and cellulase (Fig. 4).

#### Yields of BC prepared using different culture media

Corn cob hydrolysate also contains furfural, HMF, and lignin besides sugars (Table 2), which have an inhibitory effect on both the metabolism of kombucha bacteria and the BC yield (Liu et al. 2017a; Yoshioka et al. 2018). This is probably due to the interference of lignin with the cell membrane through its functional groups and changes in its protein-to-lipid ratio (Leif et al. 2013). Undissociated acids enter the cell by diffusion across the cell membrane and then dissociate due to the neutral cytosolic pH. The dissociation of acid leads to a decrease in intracellular pH, causing cell death. This impact is intensified by furfural and HMF due to their higher permeability

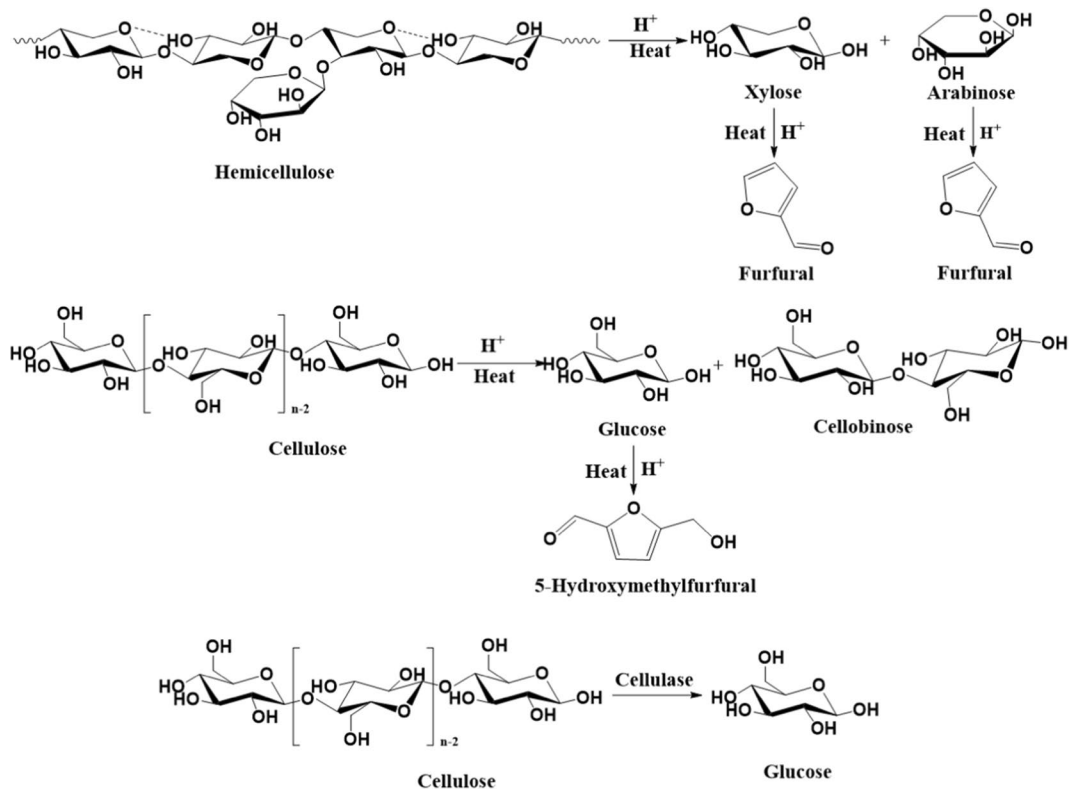


**Fig. 4** Scheme showing the mechanism of hydrolysis of corncob



**Table 2** Compositions of culture media

HS Constituent	Content (g/L)	Untreated CC Constituent	Content (g/L)	AC-treated CC Constituent	Content (g/L)	Removal rate(%)
Glucose	20.000	Sugar	22.700	Sugar	21.010	7.440
Peptone	5.000	Furfural	0.530	Furfural	0.460	13.210
Yeast	5.000	HMF	0.150	HMF	0.110	26.770
Na <sub>2</sub> HPO <sub>4</sub>	7.000	Lignin	0.004	Lignin	0.0008	80.000
Citric acid	1.000	Acetic acid	10.190	Acetic acid	10.100	0.880

HS, untreated CC, and AC-treated CC represent Hestrin-Schramm medium, corncob hydrolysate without active carbon treatment, and corncob hydrolysate treated with active carbon, respectively

through the cell membrane. This disturbs the proton gradient over the inner mitochondrial membrane, which prevents the duplication of ATP and finally causes cell death (Chandel et al. 2012). The presence of inhibitors in the hydrolysate, especially lignin, seems crucial for the subsequent fermentation process (Kucera et al. 2017). Thus, a detoxification reagent is required for lignin removal to improve the yield of BC. A study showed that the removal rate of lignin from lignocellulosic hydrolysate by activated carbon could reach 85% (Wang et al. 2016). This result was consistent with the results of the present study where the lignin removal rate reached 80% after activated carbon treatment (Table 2). Meanwhile, the removal rates of furfural and HMF were 13.21% and 26.77%, respectively. This could probably be due to the fact that the molecular structure of lignin was larger than those of furfural and HMF, and that it was easier for AC to capture it. The acetic acid concentration of 10.1 g/L did not change significantly after detoxification treatment, which was consistent with the pH range required for the growth of kombucha bacteria. The sugar content was 21.01 g/L after AC treatment, which was 7.44% lower than that obtained without AC treatment and could still provide sufficient nutrition for BC production.

Changes of pH value, sugar consumption and BC yield during fermentation are shown in Fig. 5. The pH value of culture media plays an important role in cell growth and BC production (Kongruang 2008). The pH value of HS, untreated CC medium, AC-treated CC medium began at 3.50, 3.13, 3.22 and decreased to 2.61, 2.70, 2.43 in the fermentation process, respectively, which was similar to the previous publications (Leonarski et al. 2021; Sharma and Bhardwaj 2019). The decrease of pH value in culture media was attributed to various organic acids produced by

bacteria, which may disturb enzyme activity and metabolic pathways during fermentation (Ye et al. 2019). The sugar consumption in HS, untreated CC and AC-treated CC medium was 52.50%, 31.72% and 48.60% on the 15th day, which was similar to the previous studies (Gaggia et al. 2018; Leonarski et al. 2021). The results showed that the yield of BC obtained from AC-treated CC medium (1.36 g/L) was higher than HS (1.13 g/L) and untreated CC (0.25 g/L) medium, which indicated that it was necessary to treat corncob hydrolysate with AC to remove lignin and corncob hydrolysate could be used as a medium for BC production.

#### FTIR and <sup>13</sup>C NMR analyses

FTIR spectroscopy is an important tool to determine the presence of different functional groups and the nature of chemical bonding in molecules. The spectra of BC produced using HS medium, untreated CC medium, and AC-treated CC medium are shown in Fig. 6a. The spectra showed a broad absorption peak at 3340 cm<sup>-1</sup>, attributed to the stretching vibrations of intra-chain and inter-chain -OH groups, which was in agreement with previous observations (Salama and El-Sakhawy 2016). This peak was broader in the case of BC prepared from AC-treated CC medium, as compared to those of BC products produced from HS medium and untreated CC medium suggesting a higher number of -OH groups. The peak at 2900 cm<sup>-1</sup> was consistent with the symmetric and anti-symmetric C-H stretching vibrations of CH<sub>2</sub> groups (Leonarski et al. 2021). The peak at 1430 cm<sup>-1</sup> was ascribed to the in-plane bending vibrations of -CH, further confirming the presence of the CH group (Xu et al. 2022). Peaks for the stretching vibrations of C-OH and C-O-C groups appeared

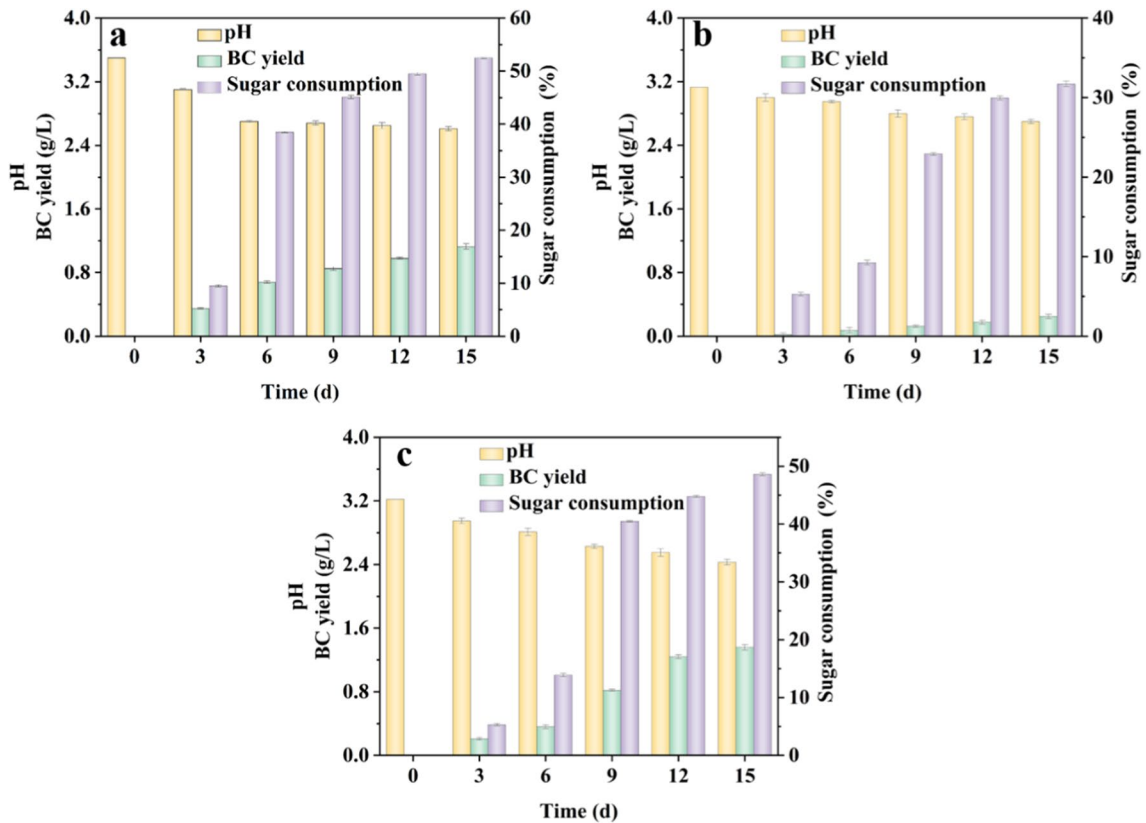


**Fig. 5** Changes in pH, BC yield and sugar consumption of different media during fermentation. **a** HS medium; **b** untreated CC medium; **c** AC-treated CC medium

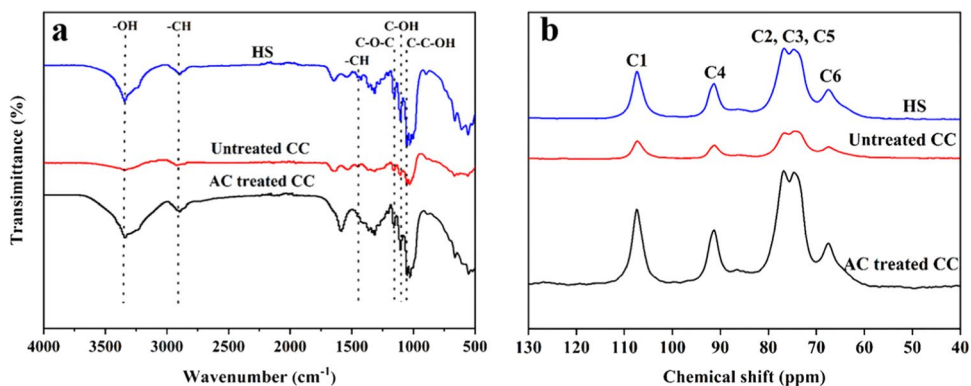


**Fig. 6** FTIR analysis of functional groups in BC (**a**) and CP/MAS  $^{13}\text{C}$  NMR spectra of BC (**b**)

in the  $1163\text{--}1000\text{ cm}^{-1}$  region. The absorption peaks at  $1160\text{ cm}^{-1}$ ,  $1110\text{ cm}^{-1}$ , and  $1059\text{ cm}^{-1}$  could be attributed to the stretching vibrations of C-O-C, C-OH, and C-C-OH bonds in secondary and primary alcohols, respectively (Lin et al. 2022). The

spectra of BC produced from untreated CC medium and AC-treated CC medium exhibited peaks similar to those of BC obtained from HS medium. These results were consistent with the basic structure of cellulose, which was also similar to the structure found

in cellulose produced by other BC-producing bacteria like *Acetobacter* (Nie et al. 2022).

The structural framework of BC was studied by  $^{13}\text{C}$  NMR spectroscopy as shown in Fig. 6b. The peaks were labeled as C1–C6, which represented the different species of C in the structural formula of BC. The chemical shifts of C in BC products derived from three different culture media were all similar, with almost no change in their chemical shifts. Instead of a double resonance peak of  $\text{I}\beta$ , the presence of a distinct and strong resonant peak at 107.4 ppm for C1 as well as a distinct peak at 91.4 ppm for C4 proved the presence of cellulose  $\text{I}\alpha$  (Atalla and Vander-Hart 1999). Peaks for C2, C3, and C5 appeared as a resonance cluster between 76.8 ppm and 74.8 ppm (Dubey et al. 2017). Meanwhile, the resonance peak at 67.6 ppm was attributed to C6. These results were consistent with previous studies (Gao et al. 2012).

### SEM analysis

The BC products obtained from all three media showed densely arranged ultrafine fibers with a 3D network structure (Fig. 7). Significantly, the fiber strands of BC cultured by untreated CC medium showed increased coalescence, as compared to BC obtained from AC-treated CC medium and HS medium, which was due to the self-aggregation of unremoved lignin in the obtained BC (Berglund et al. 2020). To check further morphological differences, 100 BC fibers were randomly chosen and their diameter distribution and average diameters were manually calculated based on the SEM images. The BC fibers produced from HS medium had a narrow distribution range of diameter (10–80 nm), with an average diameter of 38 nm (Fig. 7a1). The binding of lignin to cellulose increased the entanglements between molecular chains and thus increased the cellulose diameter (Zhao et al. 2015). As can be seen from Fig. 7b1, the diameters BC produced from untreated CC medium had a broader range (25–225 nm), with an average fiber diameter of 61.02 nm. This was 10.4% higher than that in case of AC-treated CC (Fig. 7c1), probably due to the binding of more lignin molecules on the fibers in the case of untreated CC medium. The coefficient of variation (CV) is the coefficient of change in fiber diameter, which represents the average changes in the diameter of N number of fibers. The fiber strength decreases with an increase in diameter

variability and increases with an increase in diameter (Moradi et al. 2018). From Fig. 7, it was evident that as compared to BC produced by HS medium, BC produced by AC-treated CC medium exhibited a lower CV value (37.59%) and higher mean diameter (55.23 nm), which demonstrated a higher strength of the obtained BC. Meanwhile, the unique nanofiber network morphology of BC mimics the properties of extracellular matrix to some extent, which makes it potential to be used as a scaffold for tissue engineering (Huang et al. 2013).

### XRD analysis

The crystal structures and crystallinities of BC samples were analyzed by XRD. Figure 8 shows the XRD patterns of BC products prepared using HS medium and corncob hydrolysate. Three major peaks appeared corresponding to triclinic  $\text{I}\alpha$  crystallographic planes (100), (010), (110) and monoclinic  $\text{I}\beta$  crystallographic planes (1–10), (110), (200) of BC at d-spacing values approaching 6.0, 5.3, and 3.9 Å, respectively, which were consistent with previous studies (French 2014; Hu et al. 2018; Nie et al. 2022; Ruan et al. 2016).

Crystal allomorphs (cellulose  $\text{I}\alpha$  and  $\text{I}\beta$ ) were analyzed using the equation ( $Z = 1693d_1 - 902d_2 - 549$ ) (Wada et al. 2001), where  $d_1$  is the d-spacing of (100) reflection and  $d_2$  is the d-spacing of 010 reflections. If  $Z > 0$ , then BC is rich in  $\text{I}\alpha$  form, whereas if  $Z < 0$ , BC is rich in  $\text{I}\beta$  form. The proportions of  $\text{I}\alpha$  and  $\text{I}\beta$  in BC were calculated according to the following two equations ( $\text{I}\alpha = 56.32d_1 - 63.37d_2$ ;  $\text{I}\beta = 64.53d_2 - 55.69d_1$ ), as described by Wada et al. (2001) and Ruan et al. (2016). The results in Table 3 showed that all BC samples were  $\text{I}\alpha$ -rich, among which  $\text{I}\alpha$  content of BC produced from the untreated CC medium was the lowest. That was due to the fact that all three BC samples underwent the same purification process involving sodium hydroxide treatment. However, the BC produced from the untreated CC medium had the lowest yield. This implied that for the same quality of BC samples, BC produced from untreated CC medium was more strongly affected by sodium hydroxide than that obtained from AC-treated CC medium. In the presence of strong alkali, cellulose changes from I form to II with the breaking of intermolecular and intramolecular hydrogen bonds, thus reducing the  $\text{I}\alpha$  content (Leonarski et al. 2022).

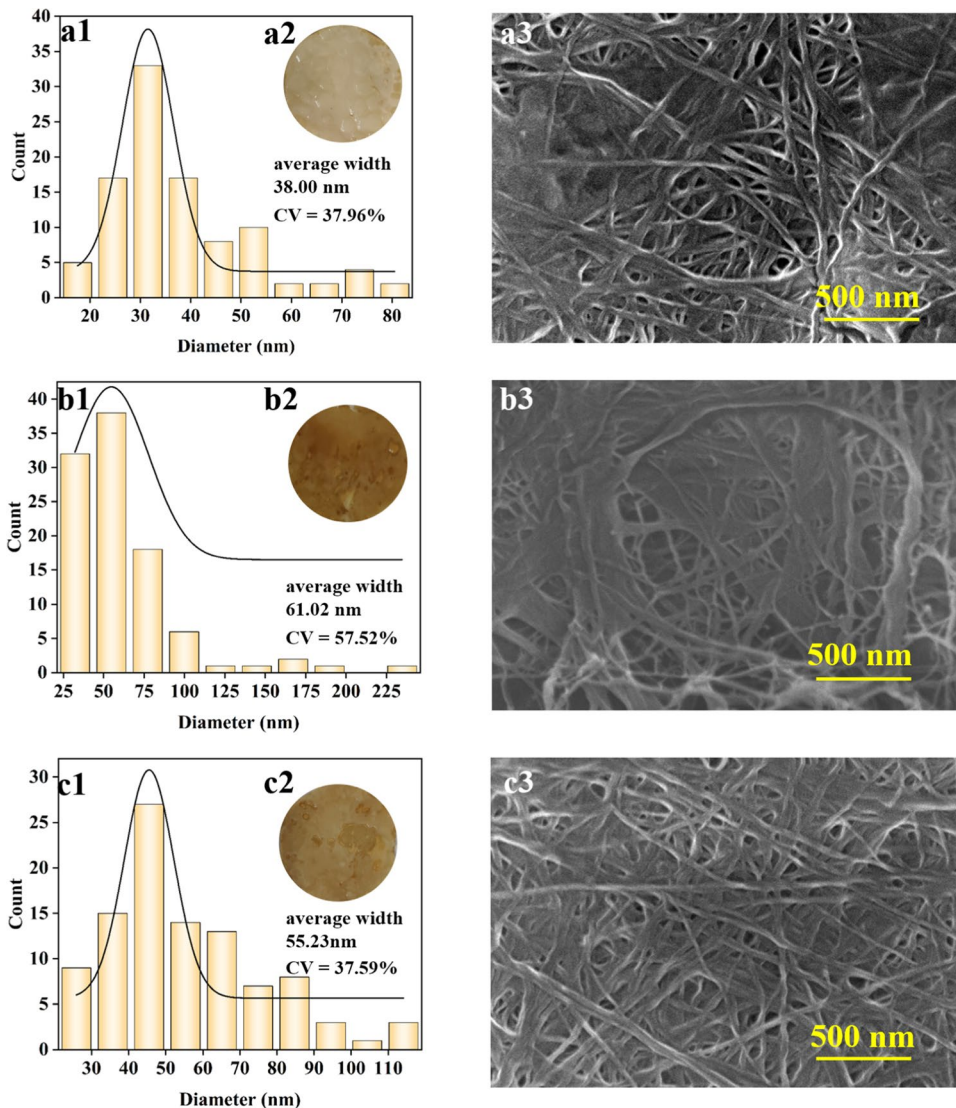


**Fig. 7** Morphological analysis of BC prepared using different media. The diameter distribution of BC fibers prepared from HS medium (a1), untreated CC medium (b1), and AC-treated CC medium (c1). The appearance of BC prepared from HS

medium (a2), untreated CC medium (b2), and AC-treated CC medium (c2). SEM of BC obtained from HS medium (a3), untreated CC medium (b3), and AC-treated CC medium (c3)

Results showed that the crystallinity of BC prepared from untreated CC medium (64.58%) decreased, as compared to BC produced by HS medium (76.79%) and AC-treated CC medium (84.65%). The components of untreated CC medium may have remained attached to the microfibrils either during or after crystallization, causing a slight decrease in crystallinity, which was consistent with previous studies (Fatima et al. 2021). Meanwhile, the

crystallinity of BC produced by AC-treated medium was 7.86% higher than that produced by HS medium. This result was consistent with the previous reports (Heydorn et al. 2023; Li et al. 2021; Lotfy et al. 2021; Nie et al. 2022; Revin et al. 2021) and suggested that BC produced by AC-treated medium had the highest proportion of crystalline regions and ordered fibrils, which were parallel to that produced by HS medium (Claudia et al. 1997). As the crystallinity of BC

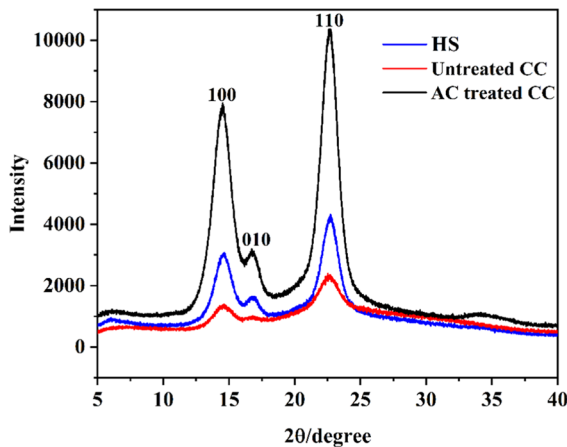


**Fig. 8** X-ray diffraction patterns of BC

produced by the AC-treated medium was not lower than that of the HS medium, BC produced by the AC-treated medium showed similar properties or applications as that of the high crystallinity of BC produced by HS medium. The fibrils of BC obtained from AC-treated CC exhibited the properties and applications of the universal crystalline cellulose, making it an ideal building block for manufacturing of strong and stiff fibers (Moon et al. 2011; Wang et al. 2017).

#### Viscosity and degree of polymerization (DP) of BC

From Table 4, the intrinsic viscosity values of BC produced from HS medium and AC-treated CC medium were 11.2 dL/g and 13.0 dL/g, respectively. Intrinsic viscosity depends on the type of solvent used, the molecular weight of the polymer, and the nature of the chemical bonding between individual monomers. Meanwhile, the higher viscosity of BC produced from AC-treated CC medium indicated the greater stiffness of the polysaccharide chain (Tsouko et al. 2015).

The DP values of BC produced from HS medium, untreated CC medium, and AC-treated CC medium

were 1709.5, 2049.9, and 2015.6, respectively. This was consistent with the results of a previous study, wherein the polymerization degree of BC prepared from beet molasses and vinasse was higher than that of HS. The reason could be that CC medium contained other sugars besides reducing sugar, which could be utilized by microorganisms not only for energy purposes but also for polymer synthesis. Meanwhile, the CC-based media was rich in compounds, such as vitamins and minerals, which could further regulate cellular processes or affect the biosynthesis of polymeric substances (Ul-Islam et al. 2015). High DPs have a positive effect on the fiber stiffness, while it undesirably influences the solubility of BC in solvents, as well as the viscosity of the spinning solution (Soares Silva et al. 2023).

#### TG and DTG analyses

The thermal stabilities of BC samples were investigated by thermogravimetric (TG) and derivative thermogravimetric (DTG) analyses, conducted in a nitrogen atmosphere, as shown in Fig. 9. The TG curves showed that the weight loss of BC produced from all three media occurred in two stages below 500 °C. The first stage with 5% weight loss occurred below 200 °C (Table 5), which was attributed to the removal of free water molecules and water molecules bonded by hydrogen bonds in the amorphous region (Khan and Park 2008). The BC samples showed good thermal stabilities, as the mass losses were less than 10% when heated up to 276 °C. In the second

**Table 4** Viscosity and degree of polymerization of BC samples

Medium	Intrinsic viscosity (dL/g)	DP
HS	11.2	1709.5
Untreated CC	13.2	2049.9
AC-treated CC	13.0	2015.6

**Table 3** Calculated crystallinities, d-spacings, Z values, and  $\alpha$  contents of crystalline phase of the produced BC from different cultivation media

Medium types	Crystallinity (%)	d-spacing (nm)			Z value	$\alpha$ content (%)
		100, $d_1$	010, $d_2$	110, $d_3$		
HS	76.79	6.08	5.28	3.91	3.19	74.20
Untreated CC	64.58	6.08	5.31	3.93	2.28	63.48
AC-treated CC	84.65	6.11	5.29	3.92	8.74	90.30



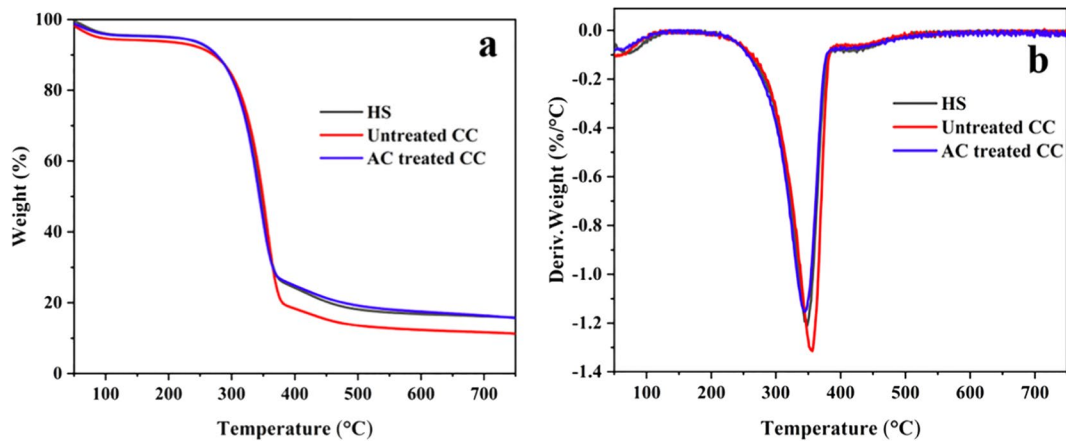


**Fig. 9** Thermal stability of BC. **a** TG curve of BC. **b** DTG curve of BC

**Table 5** Key parameters from the thermal analysis of the BC samples in a nitrogen atmosphere

Sample	T <sub>5%</sub> (°C)	T <sub>10%</sub> (°C)	T <sub>max</sub> (°C)	Residue at 750 °C (%)
HS	206	276	348	15.8
Untreated CC	88	272	358	11.3
AC-treated CC	200	276	345	15.7

stage, 71–76% weight loss occurred between 276 and 500 °C, which was due to the thermal degradation and decomposition of BC, which generated C, CO, CO<sub>2</sub>, and combustible volatiles (Machado et al. 2016). However, the peak temperature corresponding to maximum weight loss in the case of BC produced from untreated CC shifted to a higher temperature (358 °C), as compared with HS medium (348 °C) and AC-treated medium (345 °C), which was attributed to the deposition of lignin during BC production. Generally, lignin has generally higher thermal stability than that of cellulose at temperatures up to 600 °C. This slows down the decomposition process of coke formation due to the presence of aromatic groups and carbon-carbon double bonds (Trovagunta et al. 2021). BC prepared from HS medium and AC-treated CC medium exhibited similar residual carbon contents and maximum decomposition temperatures, which indicated that BC prepared from AC-treated CC medium had good thermal stability.

## Conclusions

The results of this study indicated that corncob could be a very cheap carbon source for kombucha to produce BC. It is very effective in the pretreatment of corncob to obtain optimal sugar concentration and relatively low inhibitor content to achieve an increased yield of BC. Maximum concentrations of reducing sugar and lignin were obtained from corncob on treatment with acetic acid under high pressure at 180 °C for 80 min, followed by immersion in 6 U/mL cellulase buffer solution for 24 h. Meanwhile, the BC yield from the AC-treated corncob hydrolysate medium (1.36 g/L) was higher than that from the HS medium (1.12 g/L) under optimal process conditions. FTIR spectra confirmed that BC synthesized from both HS medium and corncob hydrolysate exhibited similar chemical composition. SEM showed that BC had a 3D network structure. The BC produced by corncob hydrolysate showed a lower CV value (37.59%) and higher mean diameter (55.23 nm), as compared to the BC produced from the HS medium. XRD results showed that the crystalline structure of BC was of type I and BC produced by AC-treated CC had higher crystallinity. TG analysis demonstrated that the thermal stability of BC produced from AC-treated CC medium was as high as BC produced from HS medium. The results of this study are of great significance for the preparation of a cost-effective fermentation medium. Meanwhile, the produced BC



could be used as an alternative for natural or regenerated cellulose due to its excellent properties such as biodegradability, short production cycle and clean process, which is expected to be further applied to functional fibers or textiles.

**Author contributions** Zhanna Liu: Conceptualization, Methodology, Formal analysis, Writing – original draft. Qihang Sun: Characterization, Investigation. Yingying Wang: Methodology, Investigation. Jie Liu: Writing – review & editing. Funding acquisition. Ping Zhu: Supervision, writing – review & editing. All authors reviewed the manuscript.

**Funding** This work was financially supported by the Natural Science Foundation of Shandong Province (ZR2022QE182), State Key Laboratory of Bio-Fibers and Eco-Textiles (Qingdao University), No. TSKT202109.

**Data availability** Data will be made available on request.

#### Declarations

**Consent for publication** All authors gave their consent for publication.

**Ethics approval** This article does not contain any studies with human participants or animals performed by any of the authors.

**Competing interests** The authors declare no competing interests.

#### References

- Abdelraof M, Hasanin MS, El-Saied H (2019) Ecofriendly green conversion of potato peel wastes to high productivity bacterial cellulose. *Carbohydr Polym* 211:75–83. <https://doi.org/10.1016/j.carbpol.2019.01.095>
- Andritsou V, de Melo EM, Tsouko E, Ladakis D, Maragkoudaki S, Koutinas AA, Matharu AS (2018) Synthesis and characterization of bacterial cellulose from citrus-based sustainable resources. *ACS Omega* 3:10365–10373. <https://doi.org/10.1021/acsomega.8b01315>
- Atalla RH, VanderHart DL (1999) The role of solid state  $^{13}\text{C}$  NMR spectroscopy in studies of the nature of native celluloses. *Solid State Nucl Mag* 15:1–19. [https://doi.org/10.1016/S0926-2040\(99\)00042-9](https://doi.org/10.1016/S0926-2040(99)00042-9)
- Aung T, Eun JB (2021) Production and characterization of a novel beverage from laver (*Porphyra Dentata*) through fermentation with kombucha consortium. *Food Chem* 350:129274–129282. <https://doi.org/10.1016/j.foodchem.2021.129274>
- Babaei-Ghazvini A, Vafakish B, Patel R, Falua KJ, Dunlop MJ, Acharya B (2024) Cellulose nanocrystals in the development of biodegradable materials: a review on CNC resources, modification, and their hybridization. *Int J Biol Macromol* 258:128834–128855. <https://doi.org/10.1016/j.ijbiomac.2023.128834>
- Berglund J, Mikkelsen D, Flanagan BM, Dhital S, Gaunitz S, Henriksson G, Lindstrom ME, Yakubov GE, Gidley MJ, Vilaplana F (2020) Wood hemicelluloses exert distinct biomechanical contributions to cellulose fibrillar networks. *Nat Commun* 11:4692–4707. <https://doi.org/10.1038/s41467-020-18390-z>
- Chandel AK, da Silva SS, Singh OV (2012) Detoxification of lignocellulose hydrolysates: biochemical and metabolic engineering toward white biotechnology. *Bioenerg Res* 6:388–401. <https://doi.org/10.1007/s12155-012-9241-z>
- Chen L, Zhu JY, Baez C, Kitin P, Elder T (2016) Highly thermal-stable and functional cellulose nanocrystals and nanofibrils produced using fully recyclable organic acids. *Green Chem* 18:3835–3843. <https://doi.org/10.1039/c6gc00687f>
- Chen TY, Santoso SP, Lin SP (2022) Using formic acid to promote using formic acid to promote bacterial cellulose production and analysis of its material properties for food packaging applications. *Fermentation-Basel* 8:608–618. <https://doi.org/10.3390/fermentation8110608>
- Chen X, Ding L, Ma G, Yu H, Wang X, Zhang N, Zhong J (2023) Use of bacterial cellulose in the restoration of creased Chinese Xuan paper. *J Cult Herit* 59:23–29. <https://doi.org/10.1016/j.culher.2022.11.006>
- Chinafeed (2022) Development and market situation outlook of China's corn industry in 2022. [www.chinafeed.com.cn/yumi/202209/09/82091.html](http://www.chinafeed.com.cn/yumi/202209/09/82091.html). Accessed 9 Sept 2022
- Choi SM, Rao KM, Zo SM, Shin EJ, Han SS (2022) Bacterial cellulose and its applications. *Polymers-Basel* 14:1080–1123. <https://doi.org/10.3390/polym14061080>
- Claudia B, Daniela D, Sandra S (1997) Characterization of microbial cellulose from a high-producing mutagenized *Acetobacter pasteurianus* strain. *Biochimica et Biophysica Acta (BBA) - General Subjects* 1336(2):211–217. [https://doi.org/10.1016/S0304-4165\(97\)00030-5](https://doi.org/10.1016/S0304-4165(97)00030-5)
- Dorame-Miranda RF, Gamez-Meza N, Medina-Juarez LA, Ezquerro-Brauer JM, Ovando-Martinez M, Lizardi-Mendoza J (2019) Bacterial cellulose production by *Gluconacetobacter entanii* using pecan nutshell as carbon source and its chemical functionalization. *Carbohydr Polym* 207:91–99. <https://doi.org/10.1016/j.carbpol.2018.11.067>
- Dubey S, Sharma RK, Agarwal P, Singh J, Sinha N, Singh RP (2017) From rotten grapes to industrial exploitation: *Komagataeibacter Europaeus* SGP37, a micro-factory for macroscale production of bacterial nanocellulose. *Int J Biol Macromol* 96:52–60. <https://doi.org/10.1016/j.ijbiomac.2016.12.016>
- El-Gendi H, Taha TH, Ray JB, Saleh AK (2022) Recent advances in bacterial cellulose: a low-cost effective production media, optimization strategies and applications. *Cellulose* 29:7495–7533. <https://doi.org/10.1007/s10570-022-04697-1>
- El-Gendi H, Salama A, El-Fakharany EM, Saleh AK (2023) Optimization of bacterial cellulose production from prickly pear peels and its exsitu impregnation with fruit byproducts for antimicrobial and strawberry packaging

- applications. *Carbohydr Polym* 302:120383–120396. <https://doi.org/10.1016/j.carbpol.2022.120383>
- Fatima A et al (2021) Exsitu development and characterization of green antibacterial bacterial cellulose-based composites for potential biomedical applications. *Adv Compos Hybrid Ma* 5:307–321. <https://doi.org/10.1007/s42114-021-00369-z>
- Feng J, Zhang J, Zhang J, He Y, Zhang R, Chen C, Liu G (2017) Enhanced methane production of vinegar residue by response surface methodology (RSM). *AMB Express* 7:89–96. <https://doi.org/10.1186/s13568-017-0392-3>
- French AD (2014) Idealized powder diffraction patterns for cellulose polymorphs. *Cellulose* 21:885–896. <https://doi.org/10.1007/s10570-013-0030-4>
- French AD (2017) Glucose, not cellobiose, is the repeating unit of cellulose and why that is important. *Cellulose* 24:4605–4609. <https://doi.org/10.1007/s10570-017-1450-3>
- Gaggia F et al (2018) Kombucha Beverage from green, black and rooibos teas: a comparative study looking at microbiology, chemistry and antioxidant activity. *Nutrients* 11:11010001–11010011. <https://doi.org/10.3390/nu11010001>
- Gao SS, Wang JQ, Jin ZW (2012) Preparation of cellulose films from solution of bacterial cellulose in NMMO. *Carbohydr Polym* 87:1020–1025. <https://doi.org/10.1016/j.carbpol.2011.06.040>
- Guo J, Gu Y, Zhou X, Xu B, Wang H, Xu Y (2021) Cascade temperature-arising strategy for xylo-oligosaccharide production from lignocellulosic biomass with acetic acid catalyst recycling operation. *Renew Energy* 175:625–637. <https://doi.org/10.1016/j.renene.2021.05.066>
- Guo YW, Li CL, Li X, Xu H, Chen WC, Fang KJ, Zhang L, Li R, Xie RY (2023) Fabrication of superhydrophobic cotton fabric with multiple durability and wearing comfort via an environmentally friendly spraying method. *Ind Crop Prod* 194:116359–116370. <https://doi.org/10.1016/j.indcrop.2023.116359>
- Heydorn RL, Lammers D, Gottschling M, Dohnt K (2023) Effect of food industry by-products on bacterial cellulose production and its structural properties. *Cellulose* 4159–4179. <https://doi.org/10.1007/s10570-023-05097-9>
- Hu Y, Sheng J, Yan Z, Ke Q (2018) Completely amorphous cellulose biosynthesized in agitated culture at low temperature. *Int J Biol Macromol* 117:967–973. <https://doi.org/10.1016/j.ijbiomac.2018.06.013>
- Huang Y, Zhu C, Yang J, Nie Y, Chen C, Sun D (2013) Recent advances in bacterial cellulose. *Cellulose* 21:1–30. <https://doi.org/10.1007/s10570-013-0088-z>
- Jahan F, Kumar V, Saxena RK (2018) Distillery effluent as a potential medium for bacterial cellulose production: a biopolymer of great commercial importance. *Bioresour Technol* 250:922–926. <https://doi.org/10.1016/j.biortech.2017.09.094>
- Jesus M, Mata F, Batista RA, Ruzene DS, Albuquerque-Júnior R, Cardoso JC, Pires P, Padiilha FF, Silva DP (2023) Corn-cob as carbon source in the production of xanthan gum in different strains xanthomonas sp. *Sustainability-Basel* 15:2287–2296. <https://doi.org/10.3390/su15032287>
- Joshi SM, Gogate PR (2020) Intensification of dilute acid hydrolysis of spent tea powder using ultrasound for enhanced production of reducing sugars. *Ultrason Sonochem* 61:104843–104849. <https://doi.org/10.1016/j.ultrasonch.2019.104843>
- Jung YR, Park JM, Heo SY, Hong WK, Lee SM, Oh BR, Park SM, Seo JW, Kim CH (2015) Cellulolytic enzymes produced by a newly isolated soil fungus *Penicillium* sp. with potential for use in cellulosic ethanol production. *Renew Energy* 76:66–71. <https://doi.org/10.1016/j.renene.2014.10.064>
- Khan T, Park JK (2008) The structure and physical properties of glucuronic acid oligomers produced by a *Glucacetobacter hansenii* strain using the waste from beer fermentation broth. *Carbohydr Polym* 73:438–445. <https://doi.org/10.1016/j.carbpol.2007.12.010>
- Kongruang S (2008) Bacterial cellulose production by *Acetobacter xylinum* strains from agricultural waste products. *Appl Biochem Biotech* 148:245–256. <https://doi.org/10.1007/s12010-007-8119-6>
- Kucera D, Benesova P, Ladicky P, Pekar M, Sedlacek P, Obruca S (2017) Production of polyhydroxyalkanoates using hydrolyzates of spruce sawdust: comparison of hydrolyzates detoxification by application of overliming, active carbon, and lignite. *Bioengineering-Basel* 4(2):53–61. <https://doi.org/10.3390/bioengineering4020053>
- Kumar V, Sharma DK, Bansal V, Mehta D, Sangwan RS, Yadav SK (2019) Efficient and economic process for the production of bacterial cellulose from isolated strain of *Acetobacter pasteurianus* of RSV-4 bacterium. *Bioresour Technol* 275:430–433. <https://doi.org/10.1016/j.biortech.2018.12.042>
- Lee JW, Houtman CJ, Kim HY, Choi IG, Jeffries TW (2011) Scale-up study of oxalic acid pretreatment of agricultural lignocellulosic biomass for the production of bioethanol. *Bioresour Technol* 102:7451–7456. <https://doi.org/10.1016/j.biortech.2011.05.022>
- Leif J, Björn A, Nils-Olof N (2013) Bioconversion of lignocellulose: inhibitors and detoxification. *Biotechnol Biofuels* 6:16–25. <https://doi.org/10.1186/1754-6834-6-16>
- Leonarski E, Cesca K, Zanella E, Stambuk BU, de Oliveira D, Poletto P (2021) Production of kombucha-like beverage and bacterial cellulose by acerola byproduct as raw material. *Lwt* 135:110075–110082. <https://doi.org/10.1016/j.lwt.2020.110075>
- Leonarski E, Cesca K, Pinto CC, González SYG, de Oliveira D, Poletto P (2022) Bacterial cellulose production from acerola industrial waste using isolated kombucha strain. *Cellulose* 29:7613–7627. <https://doi.org/10.1007/s10570-022-04743-y>
- Li YM CY, Liu Y, Gao BB (2015) Evolutionary trend of China's corn output and its fluctuation characteristics based on LMDI model and EMD model. *Acta Sci Nat Univ Pekin* 51:946–954. <https://doi.org/10.13209/j.0479-8023.2015.103>
- Li ZY, Azi F, Dong JJ, Liu LZ, Ge ZW, Dong MS (2021) Green and efficient in-situ biosynthesis of antioxidant and antibacterial bacterial cellulose using wine pomace. *Int J Biol Macromol* 193:2183–2191. <https://doi.org/10.1016/j.ijbiomac.2021.11.049>
- Lin SP, Huang SH, Ting Y, Hsu HY, Cheng KC (2022) Evaluation of detoxified sugarcane bagasse hydrolysate by atmospheric cold plasma for bacterial cellulose production. *Int J*

- Biol Macromol 204:136–143. <https://doi.org/10.1016/j.ijbiomac.2022.01.186>
- Liu Y, Geng Y, Zhou Q, Yuan W (2017a) The effect of furfural and 5-hydroxymethyl furfural on butyric acid fermentation by *Clostridium tyrobutyricum*. *J Chem Technol Biot* 93:849–854. <https://doi.org/10.1002/jctb.5439>
- Liu Y, Guo L, Wang L, Zhan W, Zhou H (2017b) Irradiation pretreatment facilitates the achievement of high total sugars concentration from lignocellulose biomass. *Bioresour Technol* 232:270–277. <https://doi.org/10.1016/j.biortech.2017.01.061>
- Liu K, Jiang B, Wang Q, Yang L, Lu B, Li X, Yuan H (2020) Study on the conditions of pretreating vinegar residue with sodium hydroxide for simultaneous saccharification and fermentation to produce alcohol and xylose. *Food Sci Technol Res* 26:381–388. <https://doi.org/10.3136/fstr.26.381>
- Loffy VF, Basta AH, Abdel-Monem MO, Abdel-Hamed GZ (2021) Utilization of bacteria in rotten Guava for production of bacterial cellulose from isolated and protein waste. *Carbohydr Polym Technol Appl* 2:100076–100084. <https://doi.org/10.1016/j.carpta.2021.100076>
- Luo C, Shao Y, Yu H, Ma H, Zhang Y, Yin B, Yang M (2022) Improving the output performance of bacterial cellulose-based triboelectric nanogenerators by modulating the surface potential in a simple method. *ACS Sustain Chem Eng* 10:13050–13058. <https://doi.org/10.1021/acsschemeng.2c03189>
- Ma T, Zhao J, Ao L, Liao X, Ni Y, Hu X, Song Y (2018) Effects of different pretreatments on pumpkin (*Cucurbita pepo*) lignocellulose degradation. *Int J Biol Macromol* 120:665–672. <https://doi.org/10.1016/j.ijbiomac.2018.08.124>
- Machado RTA, Gutierrez J, Tercjak A, Trovatti E, Uahib FGM, Moreno GP, Berreta AA, Ribeiro SJL, Barud HS (2016) *Komagataeibacter rhaeticus* as an alternative bacteria for cellulose production. *Carbohydr Polym* 152:841–849. <https://doi.org/10.1016/j.carbpol.2016.06.049>
- Mbituyimana B, Liu L, Ye W, Ode Boni BO, Zhang K, Chen J, Thomas S, Vasilievich RV, Shi Z, Yang G (2021) Bacterial cellulose-based composites for biomedical and cosmetic applications: Research progress and existing products. *Carbohydr Polym* 273:118565–118574. <https://doi.org/10.1016/j.carbpol.2021.118565>
- Miller GL (1959) Use of dinitrosalicylic acid reagent for determination of reducing sugar. *Anal Chem* 31:426–428. <https://doi.org/10.1021/ac60147a030>
- Moon RJ, Martini A, Nairn J, Simonsen J, Youngblood J (2011) Cellulose nanomaterials review: structure, properties and nanocomposites. *Chem Soc Rev* 40:3941–3994. <https://doi.org/10.1039/c0cs00108b>
- Moradi S, Liu X, Najjar SS, Wang X (2018) Tensile strength prediction of irregular fibres using diameter-dependent Weibull analysis. *J Text Inst* 110:600–605. <https://doi.org/10.1080/00405000.2018.1500087>
- Nayebi M, Faraji A, Bahadoran A, Othman ZJ, Arghavani S, Kargar PG, Sajjadinezhad SM, Varma RS (2023)  $\text{TiO}_2/\text{g-C}_3\text{N}_4/\text{SO}_3\text{H}$  (IL): unique usage of ionic liquid-based sulfonic acid as an efficient photocatalyst for visible-light-driven preparation of 5-HMF from cellulose and glucose. *ACS Appl Mater Inter* 15:8054–8065. <https://doi.org/10.1021/acsmami.2c20480>
- Nie WX, Zheng X, Feng W, Liu Y, Li Y, Liang X (2022) Characterization of bacterial cellulose produced by *Acetobacter pasteurianus* MGC-N8819 utilizing lotus rhizome. *Lwt* 165:113763. <https://doi.org/10.1016/j.lwt.2022.113763>
- Ouyang DH, Liu TX, Astimar AA, Lau HLN, Teh SS, Nursyairah J, Liu D, Zhao X (2023) Model-based process intensification of dilute acid pre-hydrolysis of oil palm empty fruit bunch biomass for pretreatment and furfural production. *Bioresour Technol* 372:128626–128635. <https://doi.org/10.1016/j.biortech.2023.128626>
- Padmanabhan SK, Lionetto F, Nisi R, Stoppa M, Licciulli A (2022) Sustainable production of stiff and crystalline bacterial cellulose from orange peel extract. *Sustainability-Basel* 14:2247–2258. <https://doi.org/10.3390/su14042247>
- Pan L, Li Q, Tao Y, Ma C, Chai H, Ai Y, He YC (2022) An efficient chemoenzymatic strategy for valorisation of corncob to furfuryl alcohol in CA: betaine-water. *Ind Crop Prod* 186:115203–115213. <https://doi.org/10.1016/j.indcrop.2022.115203>
- Revin VV, Dolganov AV, Liyaskina EV, Nazarova NB, Balandina AV, Devyataeva AA, Revin VD (2021) Characterizing bacterial cellulose produced by *Komagataeibacter sucrofermentans* H-110 on molasses medium and obtaining a biocomposite based on it for the adsorption of fluoride. *Polymers-Basel* 13:1422–1437. <https://doi.org/10.3390/polym13091422>
- Ruan C, Zhu Y, Zhou X, Abidi N, Hu Y, Catchmark JM (2016) Effect of cellulose crystallinity on bacterial cellulose assembly. *Cellulose* 23:3417–3427. <https://doi.org/10.1007/s10570-016-1065-0>
- Salama A, El-Sakhawy M (2016) Regenerated cellulose/wool blend enhanced biomimetic hydroxyapatite mineralization. *Int J Biol Macromol* 92:920–925. <https://doi.org/10.1016/j.ijbiomac.2016.07.077>
- Segal L, Creely JJ, Martin AE, Conrad CM (1959) An empirical method for estimating the degree of crystallinity of native cellulose using the X-Ray diffractometer. *Text Res J* 29(10):786–794. <https://doi.org/10.1177/004051755902901003>
- Sharma C, Bhardwaj NK (2019) Biotransformation of fermented black tea into bacterial nanocellulose via symbiotic interplay of microorganisms. *Int J Biol Macromol* 132:166–177. <https://doi.org/10.1016/j.ijbiomac.2019.03.202>
- Sieborg MU, Jønson BD, Larsen SU, Vazifehkhoran AH, Triolo JM (2020) Co-ensiling of wheat straw as an alternative pre-treatment to chemical, hydrothermal and mechanical methods for methane production. *Energies* 13:4047–4065. <https://doi.org/10.3390/en13164047>
- Soares Silva FAG, Meister F, Dourado F, Gama M (2023) Regenerated bacterial cellulose fibres. *Int J Biol Macromol* 253:127310–127318. <https://doi.org/10.1016/j.ijbiomac.2023.127310>
- Trovagunta R, Zou T, Osterberg M, Kelley SS, Lavoine N (2021) Design strategies, properties and applications of cellulose nanomaterials-enhanced products with residual, technical or nanoscale lignin-A review. *Carbohydr Polym* 254:117480–117502. <https://doi.org/10.1016/j.carbpol.2020.117480>

- Tsouko E, Kourmentza C, Ladakis D, Kopsahelis N, Mandala I, Papanikolaou S, Paloukis F, Alves V, Koutinas A (2015) Bacterial cellulose production from industrial waste and by-product streams. *Int J Mol Sci* 16:14832–14849. <https://doi.org/10.3390/ijms160714832>
- Ul-Islam M, Khan S, Ullah MW, Park JK (2015) Bacterial cellulose composites: synthetic strategies and multiple applications in bio-medical and electro-conductive fields. *Biotechnol J* 10:1847–1861. <https://doi.org/10.1002/biot.201500106>
- Wada M, Okano T, Sugiyama J (2001) Allomorphs of native crystalline cellulose I evaluated by two equatorial d-spacings. *J Wood Sci* 47:124–128. <https://doi.org/10.1007/BF00780560>
- Wang Z, Zhuang J, Wang X, Li Z, Fu Y, Qin M (2016) Limited adsorption selectivity of active carbon toward non-saccharide compounds in lignocellulose hydrolysate. *Bioresour Technol* 208:195–199. <https://doi.org/10.1016/j.biortech.2016.02.072>
- Wang S, Jiang F, Xu X, Kuang Y, Fu K, Hitz E, Hu L (2017) Super-strong, super-stiff macrofibers with aligned, long bacterial cellulose nanofibers. *Adv Mater* 29:1702498–1702505. <https://doi.org/10.1002/adma.201702498>
- Way ML, Jones JE, Nichols DS, Damberg RG, Swarts ND (2020) A comparison of laboratory analysis methods for total phenolic content of cider. *Beverages* 6:55–65. <https://doi.org/10.3390/beverages6030055>
- Wen PY, Zhang T, Wei LT, Wang JY, Ragauskas AJ, Zhang Y, Xu Y, Zhang JH (2021) Effect of dilute acetic acid hydrolysis on xylooligosaccharide production and the inhibitory effect of cellulolytic enzyme lignin from poplar. *ACS Sustain Chem Eng* 9:11361–11371. <https://doi.org/10.1021/acssuschemeng.1c02937>
- Xu S, Ge X, Tan L, Liu T (2022) Low-cost and highly efficient production of bacterial cellulose from sweet potato residues: optimization, characterization, and application. *Int J Biol Macromol* 196:172–179. <https://doi.org/10.1016/j.ijbiomac.2021.12.021>
- Ye JB, Zheng SS, Zhang Z, Yang F, Ma K, Feng Y, Zheng J, Mao D, Yang X (2019) Bacterial cellulose production by *Acetobacter Xylinum* ATCC 23767 using tobacco waste extract as culture medium. *Bioresour Technol* 274:518–524. <https://doi.org/10.1016/j.biortech.2018.12.028>
- Yoshioka K, Daidai M, Matsumoto Y, Mizuno R, Katsura Y, Hakogi T, Yanase H, Watanabe T (2018) Self-sufficient bioethanol production system using a lignin-derived adsorbent of fermentation inhibitors. *ACS Sustain Chem Eng* 6:3070–3078. <https://doi.org/10.1021/acssuschemeng.7b02915>
- Yuan H, Chen L, Hong FF (2020) A biodegradable antibacterial nanocomposite based on oxidized bacterial nanocellulose for rapid hemostasis and wound healing. *ACS Appl Mater Inter* 12:3382–3392. <https://doi.org/10.1021/acami.9b17732>
- Yuan Y, Jiang B, Chen H, Wu W, Wu S, Jin Y, Xiao H (2021) Recent advances in understanding the effects of lignin structural characteristics on enzymatic hydrolysis. *Biotechnol Biofuels* 14:205–225. <https://doi.org/10.1186/s13068-021-02054-1>
- Yuan X, Cao J, Wang R, Han Y, Zhu J, Lin J, Yang L, Wu M (2023) Genetically engineering *Escherichia coli* to produce xylitol from corn cob hydrolysate without lime detoxification. *Molecules* 28:1550–1561. <https://doi.org/10.3390/molecules28041550>
- Zhang Z, Ai F, Li Y, Zhu S, Wu Q, Duan Z, Liu H, Qian L, Zhang Q, Zhang Y (2023) Co-production process optimization and carbon footprint analysis of biohydrogen and biofertilizer from corn cob by photo-fermentation. *Bioresour Technol* 375:128814–128820. <https://doi.org/10.1016/j.biortech.2023.128814>
- Zhao ZX, Tian S, Chen LH, Wang MD, Wang P (2015) Thermal performance of cellulose acetate/tea polyphenol nanofibers. *Therm Sci* 19:1327–1329. <https://doi.org/10.2298/TSCI1504327Z>
- Zhao T, Li BY, Nie K, Ben HX, Yang XL, Zhang YM, Han GT, Jiang W (2023) A novel cascade glycolic acid pretreatment-alkali degumming method for producing hemp fiber. *Ind Crop Prod* 195:116424–116431. <https://doi.org/10.1016/j.indcrop.2023.116424>

**Publisher's Note** Springer Nature remains neutral with regard to jurisdictional claims in published maps and institutional affiliations.

Springer Nature or its licensor (e.g. a society or other partner) holds exclusive rights to this article under a publishing agreement with the author(s) or other rightsholder(s); author self-archiving of the accepted manuscript version of this article is solely governed by the terms of such publishing agreement and applicable law.